SCIENCE CHINA
Information Sciences

• REVIEW •

August 2025, Vol. 68, Iss. 8, 181401:1–181401:18
https://doi.org/10.1007/s11432-025-4383-x

Recent progress and challenges of infrared quantum dots

Yin HU[1,2], Kaiyao XIN[1,2], Siqi QIU[1,3], Jianwen HU[1], Pan WANG[1], Shenqiang ZHAI[1], Guozhen SHEN[4], Juehan YANG[1*] & Zhongming WEI[1,2,3*]

[1]*State Key Laboratory of Semiconductor Physics and Chip Technologies, Institute of Semiconductors, Chinese Academy of Sciences, Beijing 100083, China*
[2]*Center of Materials Science and Optoelectronics Engineering, University of Chinese Academy of Sciences, Beijing 100049, China*
[3]*Sino-Danish College, University of Chinese Academy of Sciences, Beijing 100049, China*
[4]*School of Integrated Circuits and Electronics, Beijing Institute of Technology, Beijing 100081, China*

Received 21 February 2025/Revised 20 March 2025/Accepted 6 April 2025/Published online 9 July 2025

Abstract This review explores the recent advancements in the field of infrared quantum dot (QD) materials, focusing on their synthesis, characterization, and applications. In recent years, precise control of the physical size and modulation of the chemical components in QDs has enabled efficient and tunable photoelectric properties. The distinctive emission and absorption properties of infrared QDs indicate their importance across diverse applications. This review covers the fundamental physical properties of QDs; elucidates their regulatory mechanisms; discusses their synthesis methods; and explores their applications in photodetectors, light-emitting diodes, lasers, photovoltaic devices, and others. Finally, it addresses existing challenges and outlines prospective future opportunities in the field of infrared QD technology.

Keywords infrared quantum dots, colloidal quantum dots, physical properties, infrared optoelectronics, infrared photodetector

Citation Hu Y, Xin K Y, Qiu S Q, et al. Recent progress and challenges of infrared quantum dots. Sci China Inf Sci, 2025, 68(8): 181401, https://doi.org/10.1007/s11432-025-4383-x

1 Introduction

Ever since Moungi Bawendi pioneered the chemical synthesis method for quantum dots (QDs) in 1993 [1], a nascent field within nanomaterial research has progressively garnered the attention of researchers. In recent years, the synthesis, characterization, and application technologies of numerous QD material systems have been proven technique. Figure 1 shows these artificial semiconductor particles with the nanoscale exhibiting a unique quantum confinement effect in their electrical and optical properties. The QD bandgap increases with decreasing size, and a blue shift is observed in the spectrum [2]. In recent years, the solution method and epitaxy method have been developed. By leveraging this quantum confinement effect, the realization of efficient and tunable photoelectric properties in QD devices can be achieved through precise control of the physical size and modulation of the chemical components. The control of wave functions ensures stability [3].

Functioning as a possible adaptable material, QDs have become increasingly pervasive in the domain of information and detection technology. Especially in the field of infrared detection, they offer unique advantages. By incorporating a narrow bandgap structure, infrared QDs exhibit the capacity to absorb or emit light including the near-infrared (NIR, 0.70–1.4 μm), short-wavelength infrared (SWIR, 1.4–2.5 μm), mid-wavelength infrared (MWIR, also means mid-infrared, 2.5–25 μm), and long-wavelength infrared (LWIR, 25–500 μm) regions, according to the International Commission on Illumination classification [4]. Infrared detectors play a pivotal role in various applications, such as navigation, infrared imaging, communication technology, artificial intelligence and environmental monitoring [5–7]. The utilization of infrared QDs considerably expands the range of applications owing to the inherent advantages of facile

* Corresponding author (email: yjhyjg@semi.ac.cn, zmwei@semi.ac.cn)

© Science China Press 2025

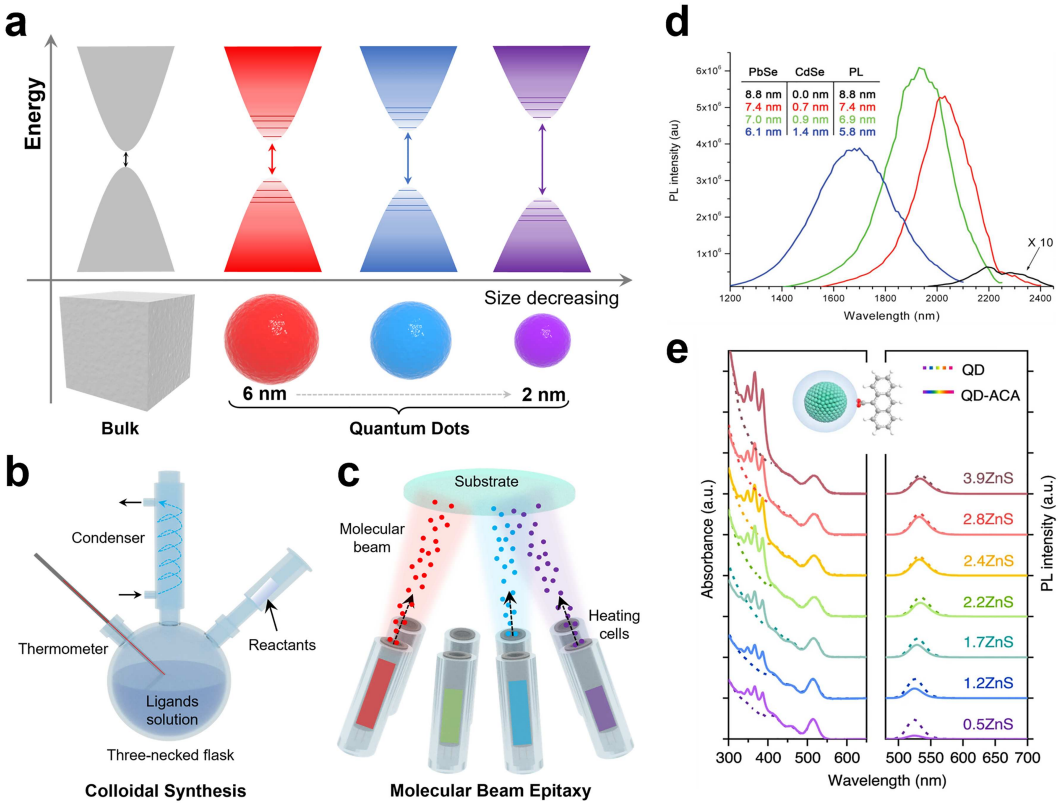

Figure 1 (Color online) Quantumconfined effects, synthesis processes and spectral information. (a) Quantum confinement effect arises when the dimensions of nanocrystals are reduced below the exciton Bohr radius of the corresponding bulk material. The bandgap undergoes widening as the particle size of the quantum dot decreases. (b) Synthesis of colloidal QDs by hot injection method. (c) Molecular beam epitaxy synthesis epitaxial QDs. (d) Blue shift occurs as the quantum dot size decreases [2] Copyright 2008 American Chemical Society. (e) Control of wave functions in CdSe/ZnS QDs with varying shell thickness (dashed line) and ACA-CdSe/ZnS QDs with 9-anthracene carboxylic acid (ACA) modification (solid line) induces photoluminescence (PL) quenching in ACA-modified QDs as the shell thickness decreases. This observation indicates a reduction in the rate of spin-triplet energy transfer with decreasing thickness [3] Copyright 2021 The Author(s).

processing, exceptional flexibility, and robust photochemical stability. The facile adjustment of QD size and structure effectively addresses the challenge of adapting target spectral responses, whereas the ordered microscale arrangement of infrared QDs provides solutions to fundamental challenges in semiconductor physics, including improving carrier migration efficiency and reducing defect density [8, 9].

Typical semiconductor groups are IV (Si, Ge, and GeSn), IV-VI (PbS, PbSe, and PbTe), III-V (InAs and InSb), II-VI (HgCdTe, HgSe, and HgTe), and I-VI (Ag_2S and Ag_2Se) [6] which is the usual component of infrared QD materials. Figure 2 shows the wavelength response range of these groups. In addition, some newly discovered perovskite QDs play a crucial role in broadening the absorption/emission wavelength of infrared QDs.

In Section 2, we first introduce the fundamental physical properties of QDs, including presenting the principle of infrared QDs, elucidating the regulatory mechanisms of infrared QDs, and expounding how to select organic ligands in colloidal QDs (cQDs). Subsequently, in Section 3, we present the intricate fabrication processes employed in QD devices. For the synthesis method of cQDs, we focus on the impact of ligand selection on the properties of cQDs. As for the epitaxy synthesis of QDs, recent advances in metalorganic vapor deposition (MOCVD) and molecular beam epitaxy (MBE) are introduced. In Section 4, we delve into the application of infrared QDs in photodetectors, light-emitting diodes (LEDs), photovoltaic devices, and other intriguing applications. Finally, in Section 5, we summarize the existing challenges while concurrently looking at prospective future opportunities in the field of infrared QDs.

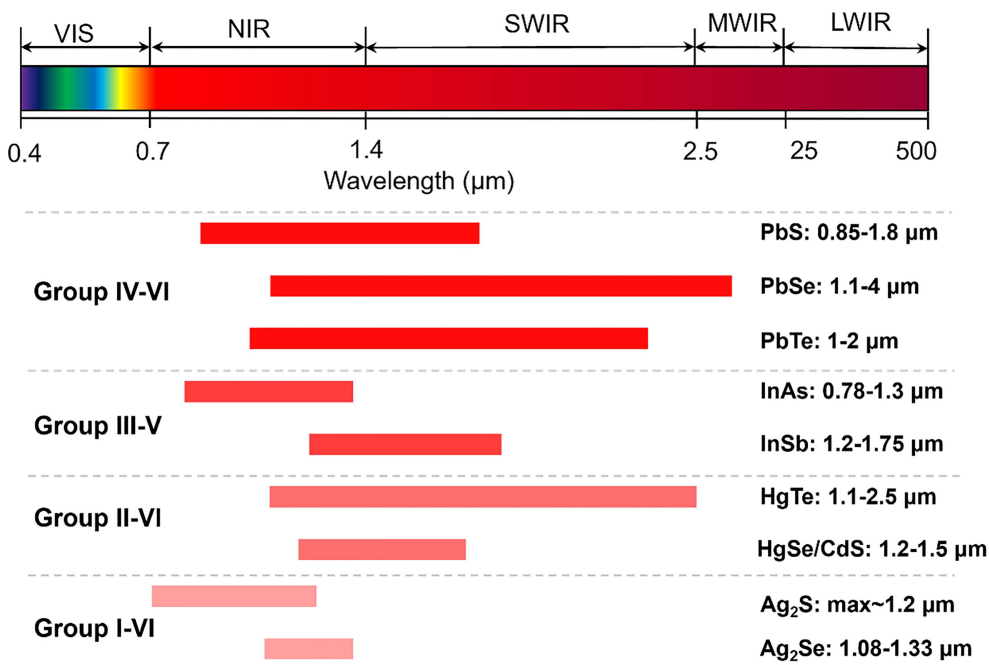

Figure 2 (Color online) Emission wavelength and bandgap energy range of representative infrared quantum dot materials.

2 Physical properties of infrared QDs

The research on QDs originated from the discovery of the quantum confinement effect [10], which occurs when the dimensions of a material are confined in space to the point where the motion of electrons is impeded. When the size of a bulk semiconductor nanocrystal diminishes to a point smaller than its exciton Bohr radius, the movement of electrons becomes localized near the Fermi level [11]. Such an appropriately sized small crystallite is referred to as a QD. As the size of the QD decreases, the quantum confinement effect intensifies, causing the conduction band and valence band to separate and increasing the effective bandgap [12]. Furthermore, this leads to a blue-shift phenomenon in the absorption and emission spectra of QDs.

This phenomenon can be described using a quantum box model by defining a spherical QD with a radius R, and its bandgap is expressed as [8]

$$E_g(\mathrm{QD}) = E_{g0} + \frac{\hbar^2\pi^2}{2m_{eh}R^2},$$

where E_{g0} is the bulk semiconductor bandgap energy and $m_{eh} = m_e m_h/(m_e + m_h)$, where m_e and m_h are the electron and hole effective masses, respectively. The sizedependent contribution to the band gap is positively correlated with $1/R^2$. For infrared QDs, reducing the size of the QD would result in a widened bandgap, and thus, it may not fall below the required infrared absorption threshold. Meanwhile, achieving the quantum confinement effect necessitates the diameter of the QD to be smaller than a few nanometers. Therefore, precise control of the QD size becomes a substantial challenge for infrared QD materials. Efficient response in the near-infrared band can be achieved by selecting heavy metal QD materials with a large exciton Bohr radius [6].

Based on the tunable band gap, four main mechanisms contribute to the use of infrared QDs in various fields as shown in Figure 3, including multiple exciton generation, biexciton gain, photoluminescence [12] and electroluminescence [13].

The tunable band is the basis of the application of QDs. In a recent report, it was evident that post synthetic surface chemistry modification, specifically through ligand exchange, plays a crucial role in influencing the optoelectronic properties of QDs. Electrostatic effects, which exist between ligands, govern the interdigitated ligands between QDs and effectively shield the ligand shell dipole. The control of absolute bandedge positions emerges as a critical design criterion for a diverse range of potential applications involving solid-state QDs and cQDs [14]. In photovoltaic solar cells, the light excitation generates photons, and as photons with energy surpassing the bandgap of the material (pn junction)

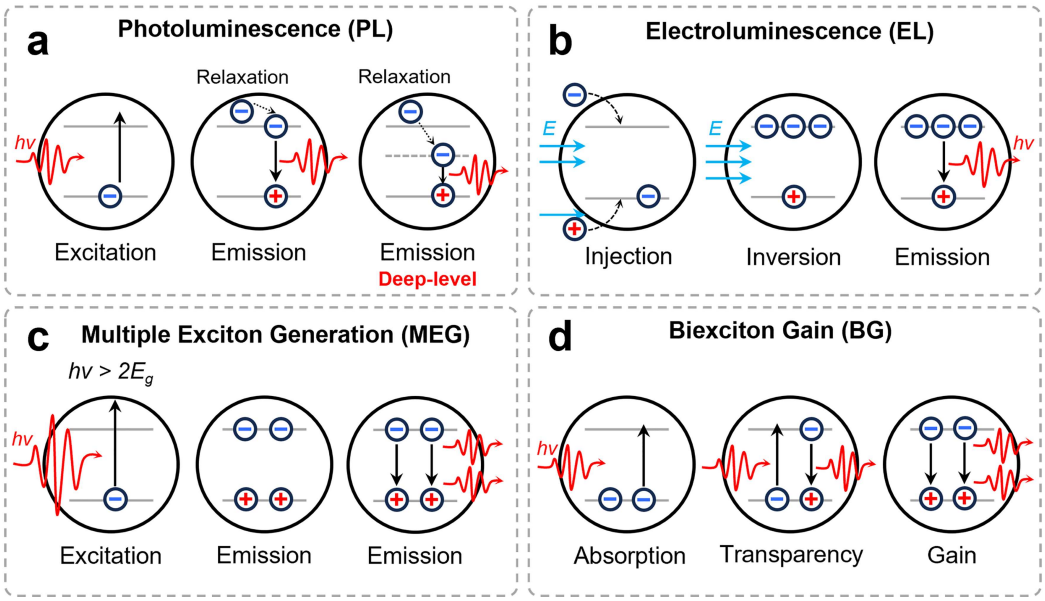

Figure 3 (Color online) Four excitation modes of QDs. (a) Photoluminescence process of QDs involves the relaxation of the electronhole pair to the eigenstate after excitation, followed by the emission of recombination light. However, the presence of a deep-level defect can lead to nonradiative recombination in this process. (b) Electroluminescence of QDs necessitates external carrier injection, with emission occurring at the interface between HTL or ETL and the active layer. (c) In the multiexciton process of QDs, high-energy photons can excite two or more excitons. (d) Double exciton optical gain process in QD lasers.

interact, electrons are extracted from the material, forming electronhole pairs. The internal electric field established by pn junctions then facilitates the separation of these pairs, leading to a current flow. Conversely, photons with energies below the bandgap do not generate electronhole pairs. Compared with bulk solar cell materials, QDs have the potential to achieve higher efficiencies. This is attributed to the bandgap tunability, which employs suitable methods to tune the absorption bandgap of QDs, covering the infrared band and enhancing the absorption of solar energy [15]. Photoluminescence is the phenomenon when an external energy, which is input in the form of incident photons on QDs causes the material to emit light at a specific wavelength. There are two main routes to describe the process of emission. QDs are one of the outstanding luminescent materials, characterized by a spectrally narrow and tunable emission line. If the transition of an electron from the valence band maximum to the conduction band minimum causes the photoelectron escape, it is referred to as band-edge emission [16]. In some cases (high temperature) excited electrons first lose energy in the form of phonons to the deep state in the band gap and then move from the deep state to the valence band by emitting photons. The mechanism of such exciton emission is complicated and needs further study. In addition, these complex mechanisms will cause nonlinear optical effects, such as QD photoluminescence under two-photon excitation [17]. The luminescence exhibited by QDs undergoes a shift corresponding to their size; smaller QDs exhibit larger band gaps. As a result, it requires more energy to excite the electrons, leading to the emission of higher-energy photons. On the contrary, designing an infrared QD requires a larger QD volume and shallow bandgap level [12]. A key parameter of QD photoluminescence is the fraction of absorbed photons that undergo re-emission by a QD, referred to as photoluminescence quantum yield (PLQY). Serving as an intrinsic property related to the single event of absorption and emission, PLQY stipulates an upper limit for the external quantum yield in luminescence color conversion facilitated by QDs [17].

The electroluminescence effect is mainly used in QD LEDs (QLEDs) and QD lasers. Unlike photoluminescence, where an external photon energy injection leads to electron transitions, electroluminescence is mainly driven by voltage, which causes electrons and holes to be injected from both ends of the electrode. Under different voltage conditions, one type of carrier passes through the QD layer and accumulates to form excitons at the interface of the hole transfer layer (HTL) or electron transfer layer (ETL) [18]. These excitons do not produce photons by radiative recombination but instead transfer energy to QDs through the Förster resonance energy transfer mechanism [13, 19]. During the formation of excitons in QLED, the effect of nonradiative recombination on device performance should also be considered. Two main aspects exist: one is the Auger recombination process between excitons and carriers. The fast relaxation of optical gain in cQDs is attributed to the nonradiative Auger recombination, and their stability

is compromised under high current densities necessary for achieving optical gain [20]. The other is the quenching effect caused by the electric field. This is owing to the luminance quenching of QDs induced by the inorganic HTL and the unbalanced charge injection resulting from a substantial energy barrier for injecting holes from HTL to QDs [21]. Efficiency and stability challenges in electroluminescent QDs have persistently arisen from two types of defects. The current optimization strategy predominantly revolves around precisely controlling the core-shell structure and adjustable energy band. Building upon this foundation, the introduction of stable charge transport materials and the optimization of the interface of each layer further contribute to addressing these challenges.

Multiple exciton generation (MEG), also known as carrier multiplication, is a process that generates two or more electronhole pairs from the absorption of a high-energy photon [22], usually exceeding a value that is twice the bandgap energy. This mechanism holds great potential as a means to enhance photocurrent and overcome the limitations imposed by the Shockley-Queisser limit [23, 24]. The manifestation of the MEG effect has paved the way for the development of the next generation of solar cells and highly efficient optoelectronic devices.

Biexciton gain is a phenomenon where the absorption of a single photon leads to the generation of two excitons instead of one exciton. Biexciton gain is crucial in the context of optical amplification and lasing applications. In QD laser applications, the gain medium amplifies light through the process of stimulated emission. Biexciton gain can enhance the overall gain and efficiency of the laser by providing an additional channel for the generation of excitons, contributing to population inversion required for laser operation. In the case of a twofold degeneracy of electron and hole states ($g_e = g_h = 2$), the light gain is expressed as $\langle N_{\text{gain}} \rangle = 1$. However, the band-edge state degeneracy can be greater than 2 in practically realized QDs [25]. This leads to more complex physical mechanisms and more interesting applications.

3 Synthesis of infrared QDs

The synthesis path of infrared QDs is primarily divided into two directions: solution method and epitaxy method.

3.1 Colloidal QD synthesis

The first direction involves a chemical method based on cQDs. Since its proposal in 1993 [1], a comprehensive set of theories and synthetic pathways has been developed to prepare low-cost, uniformly sized, and high-quality QD materials [25].

The growth of cQDs is based on the liquid phase synthesis of the colloidal solution. For the determined QD precursor substance and surfactant molecule (ligand) system, the size of nucleating particles can be controlled by the growth rate at different stages of crystal dynamics. The selection of different ligands and reaction precursors can alter the electronic and/or spatial structure of the molecular precursor, enabling controlled manipulation of QD stoichiometry, size, and crystalline phase. Owing to the requirements of infrared QDs on bandgap and exciton Bohr radius, they are generally categorized as groups IV-VI and II-VI semiconductor materials, among which the most classic is PbS infrared cQDs. These QDs possess a narrow band gap and a large exciton Bohr radius. Furthermore, they exhibit a good response performance in the nearinfrared range. Because the ligand binding sites of chalcogenide semiconductors are closely related to the chalcogenide elements, a large space exists for ligand selection. Compared with the abundant chalcogenide ligands of metal chalcogenide QDs, the anionic ligands of III-V QDs are considerably less. The ligand material of III-V QDs is selected to focus in the middle of the P organosilicon compound and as an organosilicon compound. A reasonable control of the size, size distribution and crystal phase of infrared QDs through the design of molecular precursors is still an important future research direction, and further exploration of the precursor-related chemical mechanisms is needed.

3.2 Epitaxial QD synthesis

For epitaxial QDs (eQDs), MBE and MOCVD have proven effective for synthesizing high-quality QDs on wafers [26,27]. In comparison with the colloidal chemical method, vapor phase synthesis is not constrained by the boiling point temperature of a specific solvent. This flexibility allows for a broader temperature scale to be chosen and controlled during the QD molding process. The growth of InN QDs is achieved by

MOCVD technology. A C-plane (0001)GaN layer is deposited before growth, and Si is doped on top of it. It is then deposited in nitrogen with gallium triethylum and indium triethylum as group III precursors and NH_3 as group V precursors such that the dot size can be adjusted as required [28]. However, when it comes to manufacturing high-performance AS-based QDs, MOCVD technology is unfavorable and MBE is a more suitable alternative. MBE is an ultrahigh vacuum technology that precisely controls material growth, allowing the growth of high-quality and fine-structured crystal films. MBE can be divided into two types: homogeneous epitaxy and heterogeneous epitaxy. Homoepitaxy is a technique for growing crystal films on the same crystal substrate, with the same material composition and compatible lattice structure as the substrate, thereby reducing film defects. Heteroepitaxy is the technique for growing crystal films on different crystal substrates, allowing the fabrication of novel material structures with layers of different physical properties despite the challenges posed by lattice mismatch. For the growth of InAs/GaAs QDs, approaches such as interrupting the growth mode, adjusting the growth temperature, and implementing multilayer superposition can effectively improve the surface point density, but these approaches can affect the uniformity of QDs. However, by increasing the mobility of adsorbed atoms on the surface, introducing a strainreducing layer, and optimizing the growth rate, the dimensional uniformity can be substantially improved [29]. In addition, when metalorganic vapor phase epitaxy (MOVPE) is used to prepare InGaN QDs, the morphology and performance of QDs could be optimized by changing the substrate surface pattern [30]. Controlling the growth time using IMCVD to grow MoS_2 QDs is also a feasible technology [31].

3.3 Challenges and strategies for Si-compatible QD integration

The integration of infrared QDs with Si-based platforms is critical for advancing optoelectronic and quantum technologies. However, this integration faces distinct challenges depending on the QD synthesis routes.

Solution-processed cQDs (e.g., PbS and InAs) offer compatibility with low-temperature and post fabrication deposition techniques such as spin coating, inkjet printing, and dip-coating. Their ligands can be engineered as an interface with Si oxide or nitride surfaces, enabling hybrid devices such as Si photodetectors with QD-enhanced infrared sensitivity. However, challenges persist in achieving long-term stability under thermal/electrical stress and maintaining quantum efficiency when interfaced with complementary metaloxidesemiconductor (CMOS) architectures.

Epitaxially grown QDs (e.g., InAs/GaAs and InGaN) benefit from direct growth on III-V/Si heterostructures, leveraging advancements in heteroepitaxy to mitigate lattice mismatch. Techniques such as GaN-on-Si buffer layers or selective-area epitaxy enable the monolithic integration of QDs with Si photonic circuits. For instance, InAs QDs grown on Si through metamorphic buffers have demonstrated single-photon emission compatible with Si waveguides, which is a milestone for on-chip quantum communication. Nevertheless, scalability and cost remain barriers owing to the high complexity of epitaxial growth on Si substrates.

Future research will require synergistic advances in material engineering (strain-relief layers for epitaxy and robust ligand chemistry for colloids) and process innovation (hybridbonding techniques and atomic-layer deposition for encapsulation). These efforts aim to bridge the gap between QD technologies and Si manufacturing, enabling applications in scalable quantum photonics, infrared imaging, and energy-efficient optoelectronics.

4 Applications of infrared QDs

4.1 Infrared QD photodetectors

Infrared photodetectors convert light signals into electrical signals, and they are categorized into thermal detectors and photon detectors based on different conversion mechanisms [32]. Thermal detectors, which are insensitive to wavelength but power density [33], are less suitable for applications requiring wavelength cutoff characteristics [34], especially in the context of detecting specific wavelength signals. Photodetectors, based on their structural complexity, can be further classified into three main types [9]: photoconductors (PC), photodiodes (PD), and phototransistors (PT), with these types representing a progression from simple to complex structures. QD materials have emerged as promising candidates for

infrared optical sensors owing to their favorable properties such as tunable bandgap [12] and highphoto-generated carrier mobility [35–37]. In recent years, substantial advancements have been achieved in the field of infrared QD photodetectors, building upon these three basic structures.

The photoconductor device serves as the early prototype of infrared QD photodetectors, characterized by its simple structure comprising solely a QD active layer and ohmic contact electrodes at both sides. In the initial research, MBE and colloidal chemistry were employed to fabricate InAs QD and PdS cQD photoconductor devices [38, 39]. This approach successfully extended the detection wavelength range of infrared QD photodetectors. However, despite the high carrier mobility exhibited by most carriers in the photoconductor structure, the device possesses drawbacks such as high dark current and low response speeds. These limitations hinder the fabrication of high-sensitivity devices [40].

Unlike photoelectric conductors, photodiodes rely on the migration of a few carriers, considerably reducing the leakage current and speeding up the response rate. A typical photodiode comprises an ETL, an HTL, a photosensitive layer, and two electrodes. Based on the distinct semiconductor physical properties of each layer, these diodes can adopt various layered structures, such as pn junctions, Schottky junctions, and pin junctions [41]. Photogenerated carriers in the photosensitive layer of these devices undergo separation by an internal electric field and are then output through the electrodes.

The phototransistor builds on the photodiode by incorporating gate control, featuring a structure with a source, drain, gate, and dielectric layer. The channel current, flowing from the source to the drain, can be modulated through the gate. In the case of cQDs acting as the dielectric layer, the quantum confinement effect leads to a Coulomb ladder in the form of a single electron effect when a single layer of QDs contacts the graphene gate. This represents a viable approach for a novel type of QD photodiode [42].

PbS cQDs currently dominate as the primary materials in the research of infrared QDs. In the construction of infrared photodiodes utilizing PbS cQDs, ZnO thin films serve as ETL [43], enhancing the performance by mitigating detrimental H_2O adsorption at the ZnO/PbS cQDs interface [44]. Addressing the low carrier mobility in the HTL is crucial for optimizing the response speed of the photodiode. A developed approach using NiO_X as HTL demonstrates a fourfold reduction in the photodiode response time [45]. This strategy of defect passivation and increased HTL carrier mobility is beneficial for other QDs with different components. For instance, a method that incorporates a combination of X-type methyl ammonium acetate (MaAc) and Z-type ligands $InBr_3$ is devised for InAs QDs [46], improving interface performance by passivation while maintaining carrier mobility. This results in a 25% reduction in Stokes shift and a twofold increase in photoluminescence (PL) lifetime.

For QDs used for long-wavelength infrared photodetection such as HgTe, the issue of hot carriers requires careful consideration. The quantum confinement effects in three dimensions of QDs can alleviate electron heat production, making QD materials a promising choice for achieving higher detection rates in the MWIR or LWIR detectors. A pin junction photodiode that incorporates multilayer HgTe prepared through the QD gradient homojunction method (Figures 4(a)–(c)) can yield an infrared photodetector with excellent responsivity at elevated operating temperatures [47]. The relationship between carrier diffusion length and temperature is influenced by various photosensitive aspects. The increase in carrier density at room temperature (300 K) leads to a shortened carrier lifetime, emphasizing the importance of reducing the photosensitive area to minimize the series resistance and alleviate the carrier diffusion length requirements [48]. High-sensitivity boron (B)-doped Si QD/HgCdTe (MCT) mid-infrared (MIR) photodetectors exhibit exceptional performance, with plasmon-induced hot-hole tunneling and enhanced light absorption leading to a specific defectivity of approximately 1.6×10^9 cm·Hz$^{1/2}$·W^{-1} (Jones) and fast response time (224-ns rise time and 580-ns fall time) at room temperature [49].

Infrared QDs can be used in diverse applications in infrared imaging. A dual-band detector, utilizing HgTe QDs of varying sizes (Figures 4(d)–(f)), has been demonstrated, offering rapid switching between short-wave and mid-infrared with modulation frequencies up to 100 kHz, controlled by bias polarity and amplitude [50]. In addition, nontoxic QD materials such as Ag_2Te [51], InSb [52], and Cu-In-Se [53] QDs have gained prominence in infrared imaging owing to reduced heavy metal elements, contributing to areas such as flexible electronics, bioimaging, clinical medicine, and safer consumer electronics devices.

Photodiodes typically adopt a vertical structure, and the development of transparent electrodes with selective light transparency holds critical importance for enhancing the performance of top-illuminated photodetectors. A heterojunction photoconductor, comprising transparent indium gallium zinc oxide (IGZO) and a PbS QD layer, exploits IGZO to generate a large photocurrent, resulting in an increase of several orders of magnitude in photocurrent without introducing additional noise [54]. In addition, a two-dimensional (2D) titanium carbide ($Ti_3C_2T_x$) MXene film serves as an efficient transparent con-

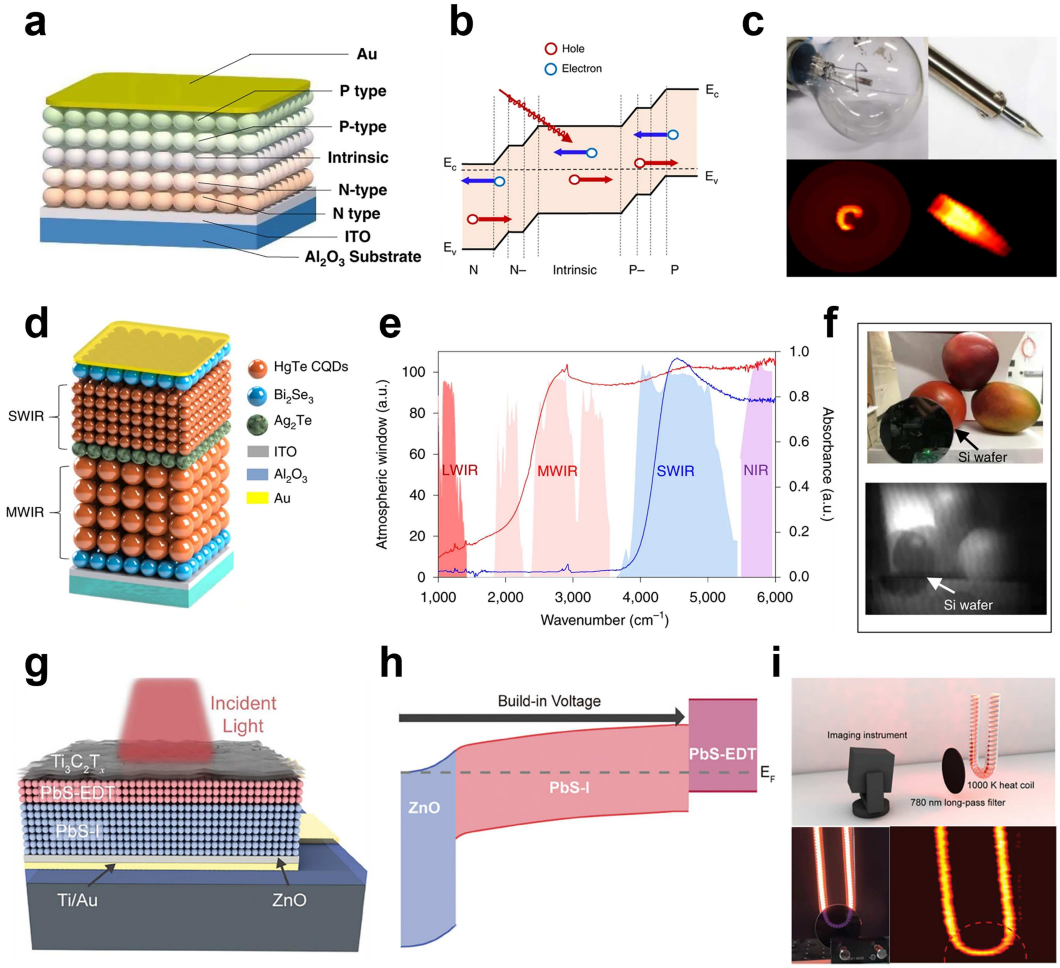

Figure 4 (Color online) (a) Schematic of pin type HgTe QDs gradient homojunction photodiode. (b) Energy diagram of mobility PIN gradient. (c) Thermal imaging diagram [47] Copyright 2023 The Author(s). (d) Schematic of dualband HgTe/Ag_2Te QD photodiode. (e) Wavelength response range of dualband photodiode. (f) Dual-band detection of hidden objects [50] Copyright 2019 The Author(s). (g) Schematic of toplighting $Ti_3C_2T_x$/PbS cQD NIR photodiode. (h) Energy level alignment in the thermal-equilibrium state. (i) Photodiode in a self-powered state exhibits similar thermal imaging results with a filter [55] Copyright 2023 The Authors.

ducting electrode for the PbS cQD photodiode (Figure 4(g)) because it offers controllable near-infrared transmittance. The device demonstrates notable characteristics, including a high specific defectivity of 5.51×10^{12} cm·W^{-1}·Hz$^{1/2}$, an extensive dynamic response range of 140 dB, and a substantial bandwidth of 0.76 MHz at 940 nm while in the self-powered state [55].

The integration of infrared cQDs with Si substrate or Si-based devices has led to the development of the infrared CMOS image sensor featuring the Si:cQD heterojunction [56]. Theoretical simulation results demonstrate that near-infrared (NIR) illumination induces changes in electrostatic potential levels within the cQD-Si heterojunction photodiode, facilitating readout through external Si-based circuits. A highly sensitive NIR photodiode has been achieved using lead PbS cQDs through multi-interface engineering, demonstrating low noise levels and high responsivity [57]. A new research direction involves the growth of a high-quality III-V epitaxial layer for MIR InGaAs/GaAs submonolayer QD quantum cascade detectors on Si, achieving an operating temperature exceeding 150 K [58].

Bandgap tunability and exciton Bohr radius are the two main factors considered in the application of infrared QD photodetectors. Infrared QDs derive their wavelength selectivity from their size-dependent bandgap, enabling precise tuning across the NIR, SWIR, and MWIR/LWIR regimes. Solution-processed QDs (e.g., PbS and HgTe) exhibit quantum confinement effects, where reducing the QD size increases the bandgap energy. For example, PbS QDs can be tuned from ∼100 nm (bulklike) to ∼2500 nm by shrinking their diameter from 8 to 3 nm [12]. Smaller QDs suffer from surface defect states because of high surface-to-volume ratios, increasing the dark current [40]. Ligand engineering (e.g., $InBr_3$/MaAc

for InAs QDs [46]) is critical to passivate traps and maintain tunability. The lattice mismatch between QDs and substrates (e.g., InAs-on-Si) introduces dislocations, thereby degrading carrier mobility [29]. Strain-reducing layers and buffer architectures (e.g., GaN-on-Si [30]) are employed to mitigate this.

The exciton Bohr radius (a_B) determines the spatial extent of electronhole pairs and dictates the degree of quantum confinement. QDs with radii smaller than a_B exhibit strong confinement, altering recombination kinetics and carrier transport. Photoconductors favor materials with a large a_B (e.g., PbS) to maximize carrier mobility. However, weak confinement increases the dark current, necessitating advanced architectures such as graded homojunctions (e.g., HgTe multilayer devices [47]). Photodiodes require precise control of a_B to balance carrier extraction (enhanced by confinement) and leakage (aggravated by surface defects). For example, InAs QDs with $InBr_3$ ligands reduce the Stokes shift by 25% through the improved confinement uniformity [46]. Phototransistors leverage gate-tunable quantum confinement (e.g., graphene-PbS interfaces [42]) to amplify photocurrent while suppressing noise.

4.2 Infrared QD light-emitting diode

Infrared QLEDs primarily rely on the electroluminescence characteristics. Similar to a pn junction diode, the emission mechanism involves carrier injection into the ETL and HTL regions under forward bias. Upon carrier recombination at the interface, photon emission occurs with an energy approximately equal to the band gap of the emission layer [59]. While visible light QLEDs with a broader color gamut and superior color accuracy have greater value than infrared QLEDs [60], infrared QLEDs play a key role in applications such as optical biomedical imaging [61], optical communication [38] and other applications [62]. As more applications are developed, the role of infrared QLEDs is expected to become more critical.

Typical infrared cQDs are selected from groups IV-VI (PbS and PbSe) [63, 64], II-VI (HgTe and CdHgSe) [65–67], and III-V (GaAs, InGaAs, InAs, InP and InSb) [52, 68]. In contrast to cQDs, the epitaxial heterostructures of III-V compounds are also commonly seen in infrared QLEDs [69].

In QLEDs, cQDs are often positioned between ETL and HTL. The crucial parameter, external quantum efficiency (EQE), is affected by issues such as interlayer defects, causing an imbalance in electron and hole injection. This imbalance results in hot electrons and hot holes with excess kinetic energy, and unstable heat excitons form through Coulomb interaction, promoting nonradiative Auger recombination and substantially impacting EQE [70].

Currently, multiple regulatory measures are employed to maintain high EQE in QLEDs. Utilizing $InBr_3$ and $SbBr_3$ halogen precursors for InSb QDs enables controlled QD diameter, impurity-free synthesis, and avoidance of secondary phases, resulting in an EQE of 10.1% [52]. The synthesis of HgTe QDs through cation exchange using Ag_2Te precursors leads to the diffusion of Ag, forming a P-doped region at one end of the HgTe active layer. The adjustment of the electronhole recombination balance was achieved by introducing a metal conductive gate to match the n-doped region at the other end (Figure 5(a)), resulting in an average power of approximately 16 μW, and the EL quantum efficiency is limited by the PL efficiency at room temperature [66]. The lattice mismatch engineering enabled by the continuous gradient in the coreshell structure of QDs initiates a reduction in interlayer lattice distortion, promoting a more uniform growth process. The high-quality shell structure diminishes interlayer defects, thereby enhancing EQE. Recently, several studies have reported $CdSe/Cd_xZn_{1-x}Se/ZnSe/ZnSe_yS_{1-y}$ [67] and In(Zn)As/In(Zn)P/GaP/ZnS [68] core/multishell heterostructures representatively. Figures 5(c)–(e) show the giant In(Zn)As/In(Zn)P/GaP/ZnS core/multishell heterostructures intense photoluminescence at approximately 850 nm. Infraredamplified spontaneous emission was observed using more ultrathin nanocrystals as the emission layer gain medium including CdHgSe/ZnCdS core/shell nanoplatelets [65] and ZnO/PbS binary blends [71]. The formation of an inorganic shell during synthesis by developing an in situ trimethylsilyl bromide (TMSBr) addition method (Figure 5(f)) would improve the carrier mobility, and the passivated QD would no longer be affected by the thickness of the emission layer [72].

Metal halide perovskites present an alternative option for infrared LEDs as they showcase noteworthy characteristics such as high PLQY, tunable compositions, and narrow emission line widths [73]. The implementation of a hole-transporting polymer with a shallower ionization potential has been shown to enhance device charge balance, efficiency, and reproducibility. Utilizing an $ITO/ZnO/PEIE/FAPbI_3$/poly-TPD/MoO_3/Al device structure, a 799-nm near-infrared PeLED has been reported to operate with an impressive EQE of 20.2% [74].

The integration of the multifunctional molecule 2-(4-(methylsulfonyl)phenyl)ethylamine helps eliminate nonradiative regions in perovskite films and suppress luminescence quenching at the interface with charge

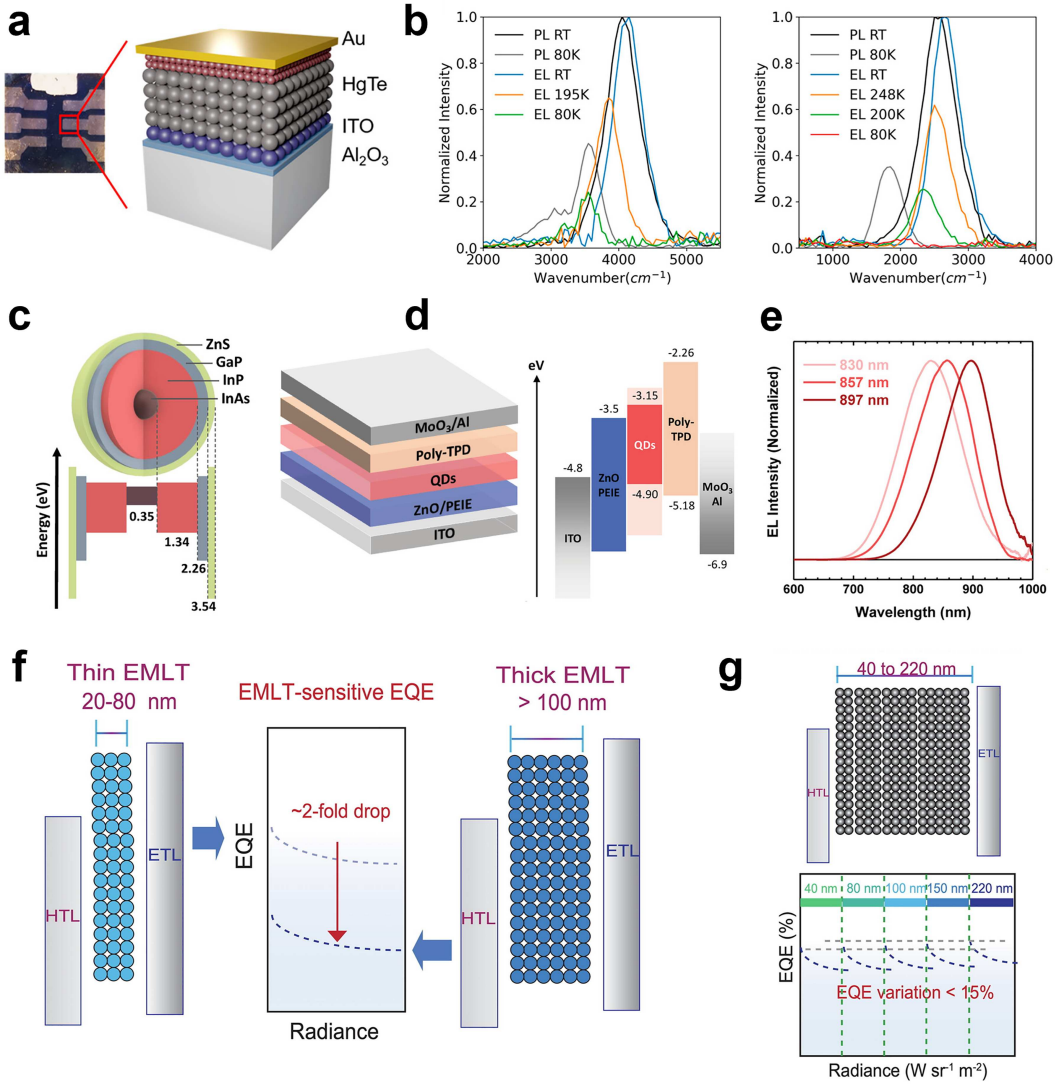

Figure 5 (Color online) (a) Schematic of the HgTe QD EL device with a metal conductive grid. (b) Short and mediumwave devices maintain the same current PL and EL spectra at different temperatures, and the EL quantum efficiency is limited by the PL efficiency at room temperature [66] Copyright 2022 American Chemical Society. (c) Multishell structure of In(Zn)As/In(Zn)P/GaP/ZnS QDs with bulk semiconductor bandgaps of the respective layers. (d) Schematic of integrated QD LED device layer structure and energy level of each layer. (e) EL spectra of QD LEDs tuned to different wavelengths [65] Copyright 2023 The Author(s). (f) Schematic of EQE sensitivity to emission layer thickness for thin and thick films in the literature. (g) Schematic of EQE insensitivity to emission layer thickness [72] Copyright 2023 Science China Press.

transport layers. This has led to the development of LEDs emitting near-infrared light at 800 nm, exhibiting a peak EQE of 23.8% at 33 mA·cm^{-2}. Moreover, these LEDs maintain EQEs exceeding 10% even at high current densities of up to 1000 mA·cm^{-2} [75].

4.3 Infrared QD lasers

Regarding the emission properties of QDs, in addition to LEDs, lasers stand out as one of the other extensively employed applications. Similar to other lasing media, achieving optical gain in nanocrystals necessitates population inversion. In this context, population inversion refers to the state in which the number of electrons in the excited state exceeds that in the ground state [76]. To achieve optical gain for infrared QDs, net stimulated emission requires biexciton states or multiple exciton states with more excitons [77]. This depends on the relation between the Stark shift (Δ_S) and the transition line width (Γ). When the magnitude of Δ_S is similar to or exceeds Γ, it has the potential to entirely eliminate the absorption losses at the emission wavelength in excited nanocrystals. But when $\Delta_S \gg \Gamma$, it is more suitable for single excitons condition [78].

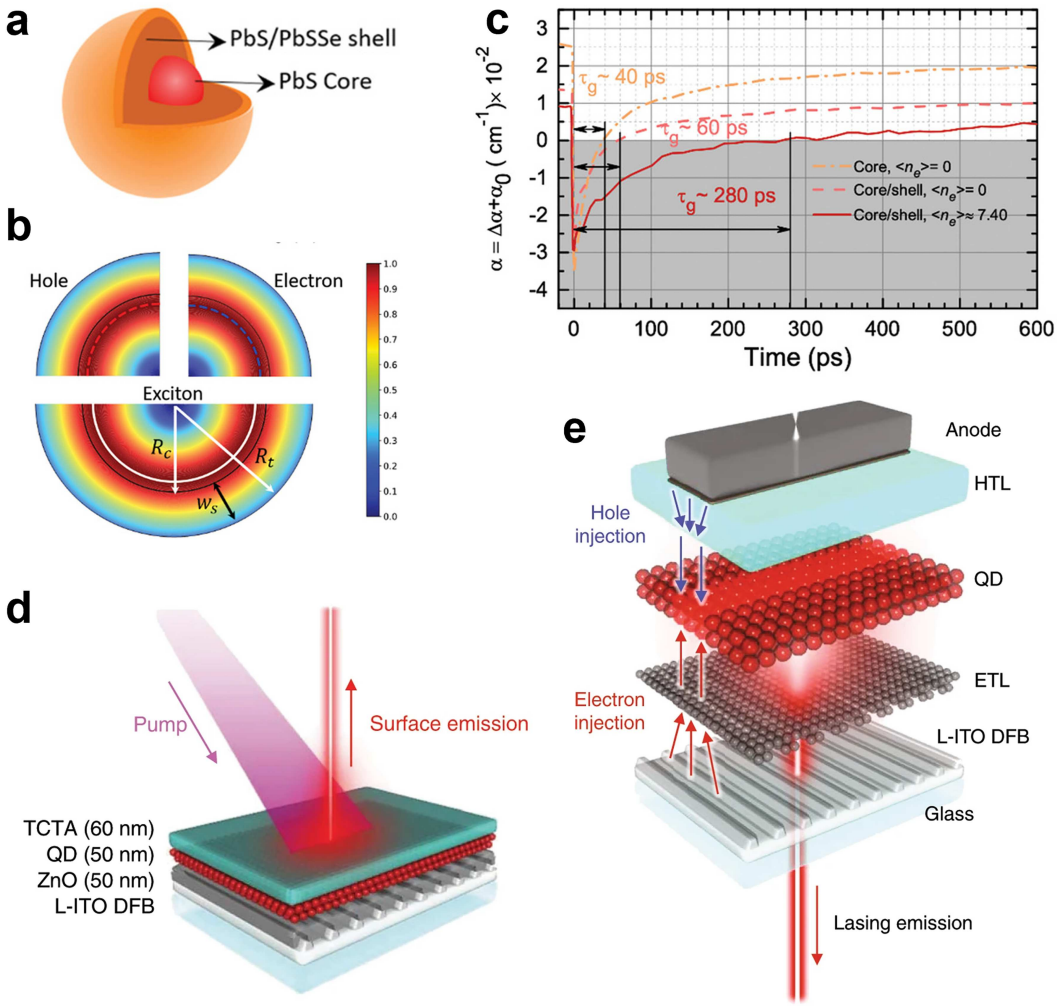

Figure 6 (Color online) (a) Schematic of the PbS/PbSSe core/alloyed-shell (C/A-S) QD structure. (b) Radial overlap density function of the electron and hole, with the solid white line indicating the maximum value. (c) Amplified spontaneous emission (ASE) peak position for undoped core, undoped C/A-S, and doped C/A-S QDs, C/A-S doping extends the optical gain life from 10 to 280 ps [82] Copyright 2022 Wiley-VCH GmbH. (d) Schematic of an optically pumped multilayered distributed feedback (DFB) laser employing the same device architecture as a traditional pin QD LED. (e) Pin-type electroluminescence QD LED with DFB cavity [88] Copyright 2020 The Author(s).

In the practical application process, the main problem that it encounters is that the cQDs synthesized by the hot solution injection method typically exhibit a weak luminescence efficiency [79]. The direct synthesis of QDs is accompanied by the emergence of a substantial number of defect states during their utilization. These defects play a key role in the rapid Auger recombination process, and the multiple exciton states experience a sharp decline in light gain owing to the Auger recombination. To overcome this limitation, defect passivation and modification of the core-shell structure can be implemented [80]. In recent years, progress in the development of infrared QD lasers has expanded to encompass applications such as multiple complex core structures, enhancements in electric pumping, and quantum cascade lasers.

By leveraging the diverse range of chalcogenide ligands [81], the engineering of core-shell structures using group IV-VI materials is recognized as an effective method for passivating infrared cQDs. The incorporation of large-scale core-shell QDs enhances the spatial extent of electronic wave functions and facilitates interfacial alloying, meanwhile achieving a smooth confinement potential [10]. A recent report demonstrates a subsingle-exciton infrared lasing with a record low threshold, achieved through the utilization of heavily doped PbS/PbSSe core/shell infrared cQDs (Figures 6(a) and (b)) as the gain medium, reaching a high net modal gain coefficient of 2180 cm^{-1} and longer gain lifetime (Figure 6(c)) [82]. A multiwavelength lasing in QD lasers is achieved using complex grating structures and flexible substrates, with distributed feedback cavities fabricated through interference lithography and QD films deposited by spin coating [83].

Recent reports on $M_xGe_{1-x}Te$ ternary colloidal libraries indicate their efficacy in regulating crystal phase transitions, enabling control over the switch between visible and near-infrared light in QDs. This development expands the options for cQD ligands [82].

Quantum cascade lasers predominantly depend on the QDs fabricated through on-chip epitaxy. cQDs exhibit high electroluminescence efficiency at visible wavelengths. However, when extended toward near-infrared and MIR bands, they encounter challenges in achieving strong emission and suffer from low quantum efficiency of approximately 0.1% [66]. The primary focus of epitaxial infrared QD research has largely revolved around exploiting interband transitions in group III-V QDs with high nonradiative Auger recombination prevalent [84–86]. Recent studies have reported new material systems. In contrast to traditional Si-based integrated lasers, group III-V QD photonic integrated circuits that utilize group IV elements such as germanium have successfully extended the operating wavelength beyond 8 μm, with a potential to reach up to 15 μm [58]. An interband cascade MIR InGaSb laser with highquality tunnel junctions reduces the leakage current while providing carrier recovery [87].

For infrared QD lasers, laser pumping offers more benefits, but reports exist that indicate electroluminescence-based devices are advancing and competing with on-chip integrated pump luminescence devices. By integrating a second-order distributed feedback resonator in the ITO cathode these devices also exhibit a strong electroluminescence performance under electrical pumping (Figures 6(d) and (e)) [88]. A recent study showcased intraband electroluminescence at 5 μm using n-doped coreshell HgSe-CdSe cQDs, indicating the potential of the cascade emission for small energy gap cQDs. The device achieved an EQE of 4.5% at 2 $A{\cdot}cm^{-2}$, which is similar to epitaxial quantum wellcascaded LEDs but operating at lower currents [89].

Mitigating Auger recombination at the device level is pivotal for enhancing operational stability and functionality in QD systems. Two material-driven strategies have emerged: 2D/0D hybrids [42], which exploit Dirac-cone carriers to dissipate Auger energy through ultrafast charge delocalization, and Type-II QDs (e.g., CdSe/CdTe [67]), wherein the spatial separation of electrons and holes across distinct material phases intrinsically suppresses the Auger processes. Complementing these approaches, machinelearning-enabled high-throughput screening accelerates the discovery of Auger-resistant materials—such as TMSBr ligands [72] and $M_xGe_{1-x}Te$ alloy compositions [82]—by mapping Auger kinetics to atomic-scale structural descriptors. By explicitly bridging the Auger physics with the device design, this framework underscores the importance of targeted strategies such as doping, heterostructuring, and interfacial engineering for advancing high-performance infrared QD lasers, where Auger losses dominate threshold currents and spectral linewidths.

4.4 Infrared QD photovoltaics

An essential application of infrared QD photovoltaics is to complement established solar cell technologies such as Si-based and perovskite-based cells. Solar radiation from the sun undergoes reflection, refraction, and absorption through the atmosphere before reaching the Earth's surface. The distribution of incident solar radiation on the surface can be assessed using AM1.5G as the standard spectrum [90]. The distribution of solar energy in the ultraviolet, visible light, and near-infrared light ranges is approximately 5%, 43%, and 52% [91], respectively. Si-based solar cells are constrained by the physical properties of Si, with a cutoff edge at 1100 nm, limiting their ability to fully utilize solar radiation (Figure 7(a)). Consequently, the use of QD materials becomes crucial to broaden the photosensitive band of traditional photovoltaic devices.

Lead chalcogenide QDs, such as PbS, PbSe, and PbTe, constitute a class of materials that are primarily employed in infrared QD photovoltaic devices. Ongoing research in this field predominantly concentrates on developing infrared solar cells that complement Si or perovskite-based solar cells.

To enhance the power conversion efficiency of solar devices, a QD passivation strategy is crucial for mitigating the impact of defect states [92]. Passivation is achieved through different organic ligands on the surface of QDs, where larger QDs correspond to smaller band gaps and longer absorption wavelengths. The shape of large QDs changes from an octahedron to a cubic octahedron with increasing size [93], leading to different polarities on each face and necessitating varied passivation measures (Figure 7(b)). Organic halide salt phenethyl ammonium iodide/bromine (PEAX, X = I/Br) additive ligands were employed in conjunction with traditional lead halide for passivating the (100) neutral surface of QDs. The power conversion efficiency was 12.28% at AM1.5G [94]. Further optimization involved improving the charge extraction contact through magnetron sputtering energy-levelarranged ZnO films, resulting in a

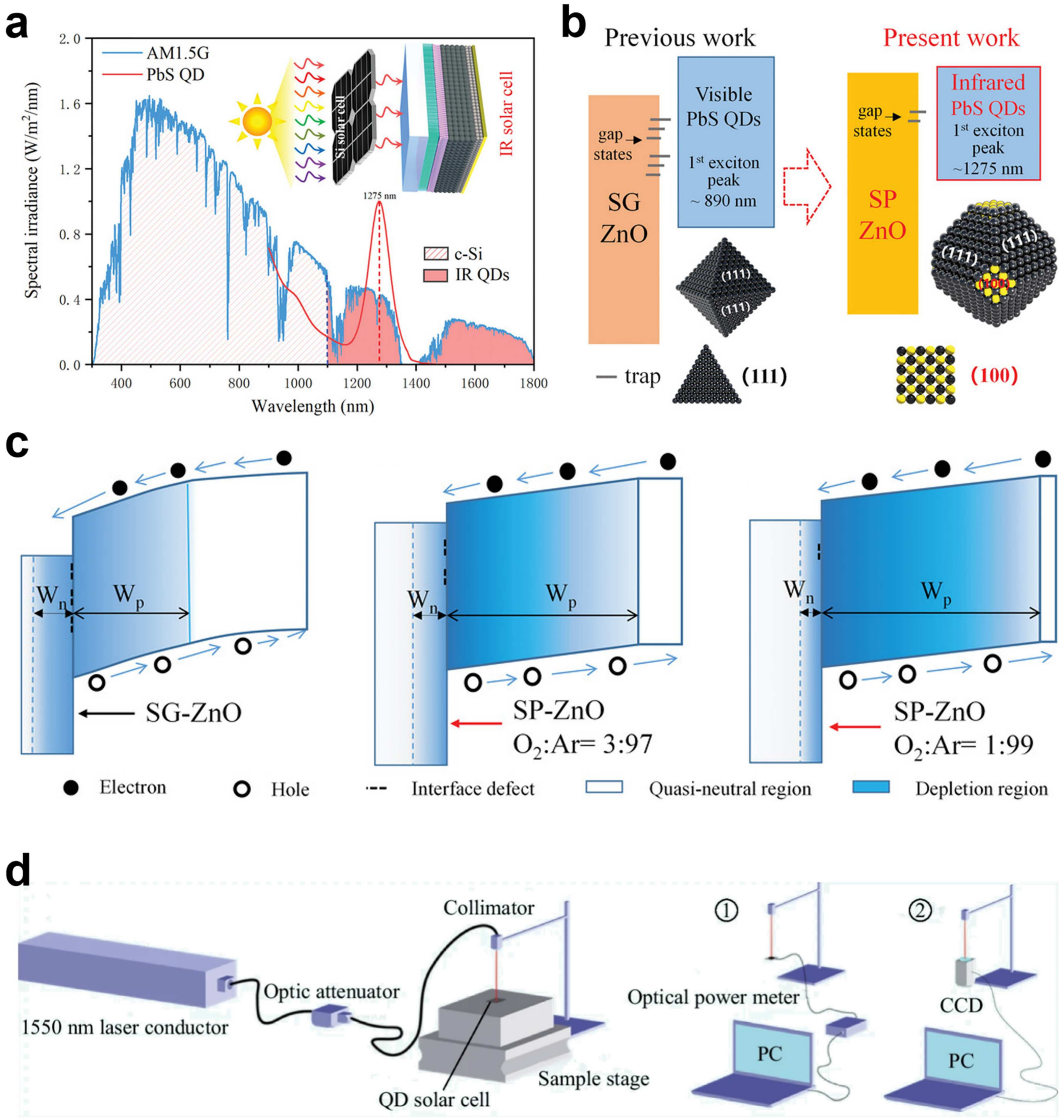

Figure 7 (Color online) (a) AM1.5G spectrum with blue curves the absorption spectrum of Si-based solar cell with grid line area and the absorption spectrum PdS QDs with red curves. (b) Schematic of energy band matching between different sizes of QDs and electron extraction ZnO layer. (c) Schematic of the depletion region, which evolves with the ZnO layer, and the optimized SP ZnO assists in widening the depletion region while suppressing interface defect-related recombination [95] Copyright 2021 Wiley-VCH GmbH. (d) Schematic of the demonstration of infrared PbS QDs in photovoltaic cells designed for wireless optical power transmission systems [96] Copyright 2023 The Author(s).

power efficiency of 10.47% [95]. Optical engineering techniques were utilized to enhance device performance, achieving a power conversion efficiency of 10.29% under 1550-nm illumination by increasing the transmittance of tin-doped indium oxide (ITO) in the infrared region and utilizing the optical resonance effect for enhanced absorption (Figure 7(d)) [96]. In addition, a hybrid passivation strategy that involves inorganic lead triiodide (PbI_3^-) and organic 3-chloro-1-propanethiol has been reported [93], leading to a 94% improvement in the power conversion efficiency of solar cells. For the PbSe structure, passivation through halide anion for Pb sites and Cd cation for Se sites considerably improved the quality of PbSe QD solar cells, achieving a 1.31% IR-PCE under 1100-nm filtered sunlight.

5 Outlook and challenges

The advancement of QD technology from maturity to large-scale applications has further expanded its importance in the field of infrared device applications, offering new solutions for the development of photoelectric devices in the infrared spectrum. This progress is multifaceted and includes the synthesis

and assembly of more efficient QDs, their integration, the development of more environmentally friendly QDs, and the exploration of more creative application scenarios for QD devices.

In particular leveraging QDs in the field of infrared technologies has made notable strides in several critical areas, enabling applications in photodetectors, QLEDs, lasers, and photovoltaics. The QDs, particularly PbS and HgTe, have become central to the evolution of infrared-sensitive devices because they offer tunable properties that enable greater sensitivity and precision in infrared detection. However, substantial challenges persist including material performance, integration with existing semiconductor technologies, and industrial scalability.

At present, various QD materials synthesized on a small scale in the laboratory confront challenges including high costs of precursor materials and potential toxicity induced by environmentally hazardous elements, especially within the infrared QD domain, wherein Cd- and Pb-based heavy metals are relied upon. The classical thermoinjection organometallic method, developed by Murray in 1992, involves highly toxic and explosive precursors such as trimethylsilyl-based chalcogenide and pnictide precursors. The substitution of these with more cost-effective and eco-friendly precursors, exemplified by oleates, ammines, or thioureas, could streamline the reaction process and substantially reduce the emission of toxic substances during the manufacturing process of QDs.

Moreover, the development of novel QD structures featuring specialized core-shell architectures will address critical issues faced by QD materials such as enhancing stability through surface passivation and doping mechanisms [97, 98], achieving band control by precise synthesis control between core-shell layers [99], and reducing toxicity by employing low-toxicity cQD precursor coordination compounds as shells. A majority of mainstream infrared QDs are derived from II-VI or IV-VI group elements, which pose critical environmental pollution challenges owing to heavy metal content under the prospect of large-scale production of cQDs. Emerging semiconductors such as I-III-VI_2 [100,101], AgS_2 [102], $CuInS_2$ [103], and Ga-based semiconductors [104] with low toxicity offer new avenues for green QD applications. However, these materials currently lack suitable precursors for synthesizing cQDs. Identifying more suitable precursor materials will open new pathways for the research of green cQDs.

In the practical application of QDs, cQD and dry-processed QD (such as epitaxial QDs) materials play vital roles. cQDs are characterized by their low cost, flexibility, and mature deployment in specific material systems. Notable examples include PbS cQDs for consumer-grade infrared imaging [51] and HgTe cQDs for long-wavelength infrared detection [47]. However, limitations such as thermal/electrical instability and dark current restrict their use in high-speed and on-chip photonic devices. For such applications, dry-processed QD materials are often preferred. Examples include InAs/GaAs eQDs for single-photon sources [58] and InGaSb QDs for quantum cascade lasers [87]. These materials exhibit superior crystallinity, compatibility with III-V/Si heteroepitaxy, and high-temperature stability, which enhance on-chip integration capabilities and broaden their application prospects. The primary challenges faced by dry-processed QDs mirror those of Si-based semiconductors, such as scalability and lattice mismatch with Si substrates [29]. Consequently, the development of dry-processed QD materials is expected to align with the evolutionary trends of traditional semiconductor materials.

In photodetection, PbS and PbSe QDs dominate infrared photovoltaics owing to their tunable bandgaps (0.7–1.3 eV), which complement the cutoff of Si at 1100 nm. Their solution processability enables lowcost and large-area deposition, while core-shell engineering (e.g., PbS/PbI_3^- hybrids [93]) mitigates defect-mediated recombination. By contrast, epitaxial InGaSb QDs [87] exhibit superior thermal stability for concentrated solar systems but face scalability barriers. Infrared photodetectors, especially those utilizing QDs, face problems such as high dark current in photoconductors and the complexities of fabricating photodiodes. Parameter optimization, particularly concerning charge transport, bandgap engineering, and interfacial characteristics, could substantially enhance the detector performance by improving sensor sensitivity and reliability. An example strategy to address these includes using ZnO films for photodetector fabrication and incorporating NiO_X as a hole transport layer (HTL) [105, 106]. However, for longer-wavelength infrared QDs (e.g., HgTe) [36], managing hot carriers—high-energy electrons that can degrade device performance—is a crucial issue that needs to be tackled for these devices to operate efficiently. Further challenges involve ensuring that QDs can be integrated seamlessly with the Si technology, which remains the dominant platform in electronic and photonic devices. Si-compatible infrared photodetectors that use QDs will be essential for large-scale commercialization, particularly for applications in sensors, communication, and imaging. Quantum-bit circuits constructed from metal oxide QDs hold the potential for exciting future applications as their strategy for sustainably controlling large-scale quantum processors by manipulating QDs in cross-structured setups may also illuminate potential development

pathways for optoelectronic applications [107].

While QLEDs have shown great promise in the infrared spectrum, challenges persist in terms of achieving high EQE, which is often affected by interlayer defects within the device structure [108]. Material defects can cause energy loss and reduce the overall brightness and efficiency of QLEDs [99]. Current strategies to overcome these challenges include the use of halogen precursors [109,110] and cation exchange processes [111] to improve the quality and performance of the QD materials. The application of strategies to suppress carrier quenching at the metal/organic interface in QLEDs can substantially enhance interface injection and transport efficiency, thereby serving as an effective solution to the problem [112]. Nonetheless, these solutions are still in development, and more research is needed to ensure long-term stability and high performance. The development of infrared QLEDs will have broad applications in telecommunications, security, and autonomous systems, where infrared light sources are crucial.

QD lasers, particularly those designed for MIR emission, are still in the developing phase, with key hurdles being material synthesis, efficient lasing, and device scalability. MIR quantum cascade lasers [113] are promising but suffer from issues such as heat dissipation and reliability when integrated with semiconductor platforms [114]. QD-based photovoltaics hold the potential for higher efficiency by extending the absorption spectrum into the infrared range, but challenges for managing hot carriers and device stability remain. The development of advanced materials, such as HgTe, PbS, and PbSe QDs [115, 116], holds promise for next-generation infrared solar cells, but the integration of these materials with current solar technologies will require overcoming critical material and process challenges. The depletion region formed at the interface between the photoactive layer and the ETL plays a crucial role in determining the performance of the device. Employing smoother surfaces to suppress interface imperfections between ETL and QDs constitutes a feasible approach [117].

The development of QD-based infrared technologies is still in the early to mid-stage of maturation, with substantial progress being made across key areas such as photodetectors, QLEDs, lasers, and photovoltaics. However, substantial challenges persist, such as material defects, device integration, and scalability. Advances in material science, particularly with respect to high-quality QDs and their integration with traditional semiconductor technologies, will be critical for overcoming these challenges. With further research and development of newer industrial solutions, there is a huge potential for QDs to revolutionize infrared technologies in fields such as communications, imaging, sensing, and energy harvesting. Future work will focus on improving device efficiency, ensuring material compatibility, and optimizing performance for further applications.

Acknowledgements This work was supported by National Key Research and Development Program of China (Grant No. 2024YFA1409700), Beijing Natural Science Foundation (Grant No. Z220005), National Natural Science Foundation of China (Grant Nos. 62125404, U24A20285, 62375256, 12304094), CAS Project for Young Scientists in Basic Research (Grant No. YSBR-053), and the 46th Research Institute of China Electronics Technology Group Corporation (Grant No. WDZC202446010).

References

1 Murray C B, Norris D J, Bawendi M G. Synthesis and characterization of nearly monodisperse CdE (E = sulfur, selenium, tellurium) semiconductor nanocrystallites. J Am Chem Soc, 1993, 115: 8706–8715
2 Pietryga J M, Werder D J, Williams D J, et al. Utilizing the lability of lead selenide to produce heterostructured nanocrystals with bright, stable infrared emission. J Am Chem Soc, 2008, 130: 4879–4885
3 Lai R, Liu Y, Luo X, et al. Shallow distance-dependent triplet energy migration mediated by endothermic charge-transfer. Nat Commun, 2021, 12: 1532
4 Ozaki Y. Infrared spectroscopy-mid-infrared, near-infrared, and far-infrared/terahertz spectroscopy. ANAL SCI, 2021, 37: 1193–1212
5 Wang P, Xia H, Li Q, et al. Sensing infrared photons at room temperature: from bulk materials to atomic layers. Small, 2019, 15: 1904396
6 Lu H, Carroll G M, Neale N R, et al. Infrared quantum dots: progress, challenges, and opportunities. ACS Nano, 2019, 13: 939–953
7 Huang Y J, Tan Y L, Kang Y, et al. Bioinspired sensing-memory-computing integrated vision systems: biomimetic mechanisms, design principles, and applications. Sci China Inf Sci, 2024, 67: 151401
8 Klimov V I. Multicarrier interactions in semiconductor nanocrystals in relation to the phenomena of auger recombination and carrier multiplication. Annu Rev Condens Matter Phys, 2014, 5: 285–316
9 Xu K, Zhou W, Ning Z. Integrated structure and device engineering for high performance and scalable quantum dot infrared photodetectors. Small, 2020, 16: 2003397
10 García de Arquer F P, Talapin D V, Klimov V I, et al. Semiconductor quantum dots: technological progress and future challenges. Science, 2021, 373: eaaz8541
11 Brus L E. Electron-electron and electron-hole interactions in small semiconductor crystallites: the size dependence of the lowest excited electronic state. J Chem Phys, 1984, 80: 4403–4409
12 Kumar D S, Kumar B J, Mahesh H M. Quantum nanostructures (QDs): an overview. In: Synthesis of Inorganic Nanomaterials. Cambridge: Woodhead Publishing, 2018. 59–88
13 Yuan Q, Wang T, Yu P, et al. A review on the electroluminescence properties of quantum-dot light-emitting diodes. Org Electron, 2021, 90: 106086
14 Kim Y, Choi M J, Choi J. Infrared-harvesting colloidal quantum dot inks for efficient photovoltaics: impact of surface chemistry and device engineering. J Mater Sci Tech, 2023, 147: 224–240

15 Uematsu T, Wajima K, Sharma D K, et al. Narrow band-edge photoluminescence from $AgInS_2$ semiconductor nanoparticles by the formation of amorphous III-VI semiconductor shells. NPG Asia Mater, 2018, 10: 713–726
16 Hu X, Zhang Y, Guzun D, et al. Photoluminescence of InAs/GaAs quantum dots under direct two-photon excitation. Sci Rep, 2020, 10: 10930
17 van Avermaet H, Schiettecatte P, Hinz S, et al. Full-spectrum InP-based quantum dots with near-unity photoluminescence quantum efficiency. ACS Nano, 2022, 16: 9701–9712
18 Mashford B S, Stevenson M, Popovic Z, et al. High-efficiency quantum-dot light-emitting devices with enhanced charge injection. Nat Photon, 2013, 7: 407–412
19 Wang T J, Cao C, Wang C. On the developments and applications of optical microcavities: an overview. Sci China Inf Sci, 2013, 56: 122401
20 Jung H, Park Y S, Ahn N, et al. Two-band optical gain and ultrabright electroluminescence from colloidal quantum dots at 1000 A cm^2. Nat Commun, 2022, 13: 3734
21 Cao F, Wu Q, Sui Y, et al. All-inorganic quantum dot light-emitting diodes with suppressed luminance quenching enabled by chloride passivated tungsten phosphate hole transport layers. Small, 2021, 17: 2100030
22 Ellingson R J, Beard M C, Johnson J C, et al. Highly efficient multiple exciton generation in colloidal PbSe and PbS quantum dots. Nano Lett, 2005, 5: 865–871
23 Li M, Begum R, Fu J, et al. Low threshold and efficient multiple exciton generation in halide perovskite nanocrystals. Nat Commun, 2018, 9: 4197
24 Shockley W, Queisser H J. Detailed balance limit of efficiency of p-n junction solar cells. J Appl Phys, 2004, 32: 510–519
25 Park Y S, Roh J, Diroll B T, et al. Colloidal quantum dot lasers. Nat Rev Mater, 2021, 6: 382–401
26 Reilly C E, Keller S, Nakamura S, et al. Metalorganic chemical vapor deposition of InN quantum dots and nanostructures. Light Sci Appl, 2021, 10: 150
27 Norman D P, Tu L W, Chiang S Y, et al. Effect of temperature and V/III ratio on the initial growth of indium nitride using plasma-assisted metal-organic chemical vapor deposition. J Appl Phys, 2011, 109: 063517
28 Reilly C E, Nakamura S, DenBaars S P, et al. MOCVD growth and characterization of InN quantum dots. Phys Status Solidi, 2020, 257: 1900508
29 Hao H M, Su X B, Zhang J, et al. Molecular beam epitaxial growth of high quality InAs/GaAs quantum dots for 1.3-μm quantum dot lasers. Chin Phys B, 2019, 28: 078104
30 Wang X, Han X, Yu J, et al. Metal-organic vapor-phase epitaxy of semipolar InGaN quantum dots based on GaN V-shaped pits. Phys Rapid Res Ltrs, 2022, 18: 2200251
31 Ahn C, Lim H. Synthesis of monolayer 2D MoS_2 quantum dots and nanomesh films by inorganic molecular chemical vapor deposition for quantum confinement effect control. Bull Korean Chem Soc, 2022, 43: 1184–1190
32 Wang Z, Gu Y, Li X, et al. Recent progress of quantum dot infrared photodetectors. Adv Opt Mater, 2023, 11: 2300970
33 Zhang S, Hu Y, Hao Q. Advances of sensitive infrared detectors with HgTe colloidal quantum dots. Coatings, 2020, 10: 760
34 Asgari M, Coquillat D, Menichetti G, et al. Quantum-dot single-electron transistors as thermoelectric quantum detectors at terahertz frequencies. Nano Lett, 2021, 21: 8587–8594
35 Imran A, He X, Liu J W, et al. Highly responsive broadband Si-based MoS_2 phototransistor on high-k dielectric. Sci China Inf Sci, 2024, 67: 160403
36 Chen M, Lan X, Tang X, et al. High carrier mobility in HgTe quantum dot solids improves Mid-IR photodetectors. ACS Photon, 2019, 6: 2358–2365
37 Chen M, Hao Q, Luo Y, et al. Mid-infrared intraband photodetector via high carrier mobility HgSe colloidal quantum dots. ACS Nano, 2022, 16: 11027–11035
38 Konstantatos G, Howard I, Fischer A, et al. Ultrasensitive solution-cast quantum dot photodetectors. Nature, 2006, 442: 180–183
39 Phillips J, Kamath K, Bhattacharya P. Far-infrared photoconductivity in self-organized InAs quantum dots. Appl Phys Lett, 1998, 72: 2020–2022
40 Konstantatos G, Sargent E H. Nanostructured materials for photon detection. Nat Nanotech, 2010, 5: 391–400
41 Konstantatos G, Sargent E H. Colloidal quantum dot photodetectors. Infrared Phys Technol, 2011, 54: 278–282
42 Fruhman J M, Astier H P A G, Ehrler B, et al. High-yield parallel fabrication of quantum-dot monolayer single-electron devices displaying Coulomb staircase, contacted by graphene. Nat Commun, 2021, 12: 4307
43 Wang H, Dong Y, Fu X, et al. Heterojunction infrared photodiodes with high dynamic range based on lead sulfide quantum dot and zinc oxide nanomembrane. IEEE Trans Nanotechnol, 2023, 22: 359–364
44 Lu S, Liu P, Yang J, et al. High-performance colloidal quantum dot photodiodes via suppressing interface defects. ACS Appl Mater Interfaces, 2023, 15: 12061–12069
45 Atan O, Pina J M, Parmar D H, et al. Control over charge carrier mobility in the hole transport layer enables fast colloidal quantum dot infrared photodetectors. Nano Lett, 2023, 23: 4298–4303
46 Xia P, Sun B, Biondi M, et al. Sequential co-passivation in InAs colloidal quantum dot solids enables efficient near-infrared photodetectors. Adv Mater, 2023, 35: 2301842
47 Xue X, Chen M, Luo Y, et al. High-operating-temperature mid-infrared photodetectors via quantum dot gradient homojunction. Light Sci Appl, 2023, 12: 2
48 Peterson J C, Guyot-Sionnest P. Room-temperature 15% efficient mid-infrared HgTe colloidal quantum dot photodiodes. ACS Appl Mater Interfaces, 2023, 15: 19163–19169
49 Cui Y Y, Tong Z Y, Zhang X L, et al. Mid-infrared plasmonic silicon quantum dot/HgCdTe photodetector with ultrahigh specific detectivity. Sci China Inf Sci, 2023, 66: 142404
50 Tang X, Ackerman M M, Chen M, et al. Dual-band infrared imaging using stacked colloidal quantum dot photodiodes. Nat Photon, 2019, 13: 277–282
51 Wang Y, Peng L, Schreier J, et al. Silver telluride colloidal quantum dot infrared photodetectors and image sensors. Nat Photon, 2024, 18: 236–242
52 Chatterjee S, Nemoto K, Ghosh B, et al. Solution-processed InSb quantum dot photodiodes for short-wave infrared sensing. ACS Appl Nano Mater, 2023, 6: 15540–15550
53 Li S, Jang J H, Chung W, et al. Ultrathin self-powered heavy-metal-free Cu-In-Se quantum dot photodetectors for wearable health monitoring. ACS Nano, 2023, 17: 20013–20023
54 Zhang C, Yin X, Chen G, et al. High-performance photodetector with a-IGZO/PbS quantum dots heterojunction. ACS Photon, 2023, 10: 790–800
55 Di Y, Ba K, Chen Y, et al. Interface engineering to drive high-performance MXene/PbS quantum dot NIR photodiode. Adv Sci, 2024, 11: 2307169
56 Xu Q, Tong X, Zhang J, et al. Near-infrared CMOS image sensors enabled by colloidal quantum dot-silicon heterojunction. Electronics, 2023, 12: 2695
57 Gong W, Wang P, Deng W, et al. Ultrahigh detectivity from multi-interfaces engineered near-infrared colloidal quantum dot photodetectors. IEEE Trans Electron Dev, 2023, 70: 3668–3674
58 Guo D, Huang J, Benamara M, et al. High operating temperature mid-infrared InGaAs/GaAs submonolayer quantum dot

quantum cascade detectors on silicon. IEEE J Quantum Electron, 2023, 59: 1–6
59 Schlotter P, Baur J, Hielscher C, et al. Fabrication and characterization of GaN/InGaN/AlGaN double heterostructure LEDs and their application in luminescence conversion LEDs. Mater Sci Eng-B, 1999, 59: 390–394
60 Tian D, Ma H, Huang G, et al. A review on quantum dot light-emitting diodes: from materials to applications. Adv Opt Mater, 2023, 11: 2201965
61 Medintz I L, Uyeda H T, Goldman E R, et al. Quantum dot bioconjugates for imaging, labelling and sensing. Nat Mater, 2005, 4: 435–446
62 Smith A M, Mancini M C, Nie S. Second window for in vivo imaging. Nat Nanotech, 2009, 4: 710–711
63 Pradhan S, Dalmases M, Taghipour N, et al. Colloidal quantum dot light emitting diodes at telecom wavelength with 18% quantum efficiency and over 1 MHz bandwidth. Adv Sci, 2022, 9: 2200637
64 Marus M, Xia Y, Zhong H, et al. Bright infra-red quantum dot light-emitting diodes through efficient suppressing of electrons. Appl Phys Lett, 2020, 116: 191103
65 Prudnikau A, Roshan H, Paulus F, et al. Efficient near-infrared light-emitting diodes based on CdHgSe nanoplatelets. Adv Funct Mater, 2024, 34: 2310067
66 Shen X, Peterson J C, Guyot-Sionnest P. Mid-infrared HgTe colloidal quantum dot LEDs. ACS Nano, 2022, 16: 7301–7308
67 Lee T, Kim B J, Lee H, et al. Bright and stable quantum dot light-emitting diodes. Adv Mater, 2022, 34: 2106276
68 Wijaya H, Darwan D, Zhao X, et al. Efficient near-infrared light-emitting diodes based on In(Zn)As-In(Zn)P-GaP-ZnS quantum dots. Adv Funct Mater, 2020, 30: 1906483
69 Vasilopoulou M, Fakharuddin A, García de Arquer F P, et al. Advances in solution-processed near-infrared light-emitting diodes. Nat Photon, 2021, 15: 656–669
70 Hanifi D A, Bronstein N D, Koscher B A, et al. Redefining near-unity luminescence in quantum dots with photothermal threshold quantum yield. Science, 2019, 363: 1199–1202
71 Taghipour N, Tanriover I, Dalmases M, et al. Ultra-thin infrared optical gain medium and optically-pumped stimulated emission in PbS colloidal quantum dot LEDs. Adv Funct Mater, 2022, 32: 2200832
72 Shen W S, Liu Y, Grater L, et al. Thickness-variation-insensitive near-infrared quantum dot LEDs. Sci Bull, 2023, 68: 2954–2961
73 Vashishtha P, Bishnoi S, Li C H A, et al. Recent advancements in near-infrared perovskite light-emitting diodes. ACS Appl Electron Mater, 2020, 2: 3470–3490
74 Zhao X, Tan Z K. Large-area near-infrared perovskite light-emitting diodes. Nat Photon, 2020, 14: 215–218
75 Sun Y, Ge L, Dai L, et al. Bright and stable perovskite light-emitting diodes in the near-infrared range. Nature, 2023, 615: 830–835
76 Klimov V I, Mikhailovsky A A, Xu S, et al. Optical gain and stimulated emission in nanocrystal quantum dots. Science, 2000, 290: 314–317
77 Geiregat P, van Thourhout D, Hens Z. A bright future for colloidal quantum dot lasers. NPG Asia Mater, 2019, 11: 41
78 Klimov V I, Ivanov S A, Nanda J, et al. Single-exciton optical gain in semiconductor nanocrystals. Nature, 2007, 447: 441–446
79 Almeida G, Ubbink R F, Stam M, et al. InP colloidal quantum dots for visible and near-infrared photonics. Nat Rev Mater, 2023, 8: 742–758
80 García-Santamaría F, Chen Y, Vela J, et al. Suppressed auger recombination in "Giant" nanocrystals boosts optical gain performance. Nano Lett, 2009, 9: 3482–3488
81 Bothra U, Albaladejo-Siguan M, Vaynzof Y, et al. Impact of ligands on the performance of PbS quantum dot visible-near-infrared photodetectors. Adv Opt Mater, 2023, 11: 2201897
82 Taghipour N, Dalmases M, Whitworth G L, et al. Colloidal quantum dot infrared lasers featuring sub-single-exciton threshold and very high gain. Adv Mater, 2023, 35: 2207678
83 Hayat A, Tong J H, Chen C, et al. Multi-wavelength colloidal quantum dot lasers in distributed feedback cavities. Sci China Inf Sci, 2020, 63: 182401
84 Haidet B B, Nordin L, Muhowski A J, et al. Interface structure and luminescence properties of epitaxial PbSe films on InAs(111)A. J Vacuum Sci Tech A-Vacuum Surfs Films, 2021, 39: 023404
85 Tournié E, Bartolome L M, Calvo M R, et al. Mid-infrared III-V semiconductor lasers epitaxially grown on Si substrates. Light Sci Appl, 2022, 11: 165
86 Deng Y, Fan Z F, Zhao B B, et al. Mid-infrared hyperchaos of interband cascade lasers. Light Sci Appl, 2022, 11: 7
87 Muhowski A J, Kamboj A, Briggs A F, et al. Cascaded InGaSb quantum dot mid-infrared LEDs. J Appl Phys, 2022, 131: 043105
88 Roh J, Park Y S, Lim J, et al. Optically pumped colloidal-quantum-dot lasing in LED-like devices with an integrated optical cavity. Nat Commun, 2020, 11: 271
89 Shen X, Kamath A, Guyot-Sionnest P. Mid-infrared cascade intraband electroluminescence with HgSe-CdSe core-shell colloidal quantum dots. Nat Photon, 2023, 17: 1042–1046
90 Tang J, Sargent E H. Infrared colloidal quantum dots for photovoltaics: fundamentals and recent progress. Adv Mater, 2011, 23: 12–29
91 Zhou R, Xu J, Luo P, et al. Near-infrared photoactive semiconductor quantum dots for solar cells. Adv Energy Mater, 2021, 11: 2101923
92 Khalaf G M G, Li M, Yan J, et al. PbS colloidal quantum dots infrared solar cells: defect information and passivation strategies. Small Sci, 2023, 3: 2300062
93 Mahajan C, Sharma A, Rath A K. Solution-phase hybrid passivation for efficient infrared-band gap quantum dot solar cells. ACS Appl Mater Interfaces, 2020, 12: 49840–49848
94 Li M, Zhao X, Zhang A, et al. Organic ligand complementary passivation to colloidal-quantum-dot surface enables efficient infrared solar cells. Chem Eng J, 2023, 455: 140961
95 Li M, Chen S, Zhao X, et al. Matching charge extraction contact for infrared PbS colloidal quantum dot solar cells. Small, 2022, 18: 2105495
96 Zhu M, Zhang Y, Lu S, et al. Optical engineering of infrared PbS CQD photovoltaic cells for wireless optical power transfer systems. Front Optoelectron, 2023, 16: 15
97 Liu M, Yazdani N, Yarema M, et al. Colloidal quantum dot electronics. Nat Electron, 2021, 4: 548–558
98 Kim J I, Lee J. Sub-kilogram-scale one-pot synthesis of highly luminescent and monodisperse core/shell quantum dots by the successive injection of precursors. Adv Funct Mater, 2006, 16: 2077–2082
99 Shin D, Park Y, Jeong H, et al. Exploring the potential of colloidal quantum dots for near-infrared to short-wavelength infrared applications. Adv Energy Mater, 2025, 15: 2304550
100 Jain S, Bharti S, Bhullar G K, et al. I-III-VI core/shell QDs: synthesis, characterizations and applications. J Lumin, 2020, 219: 116912
101 Ponomaryova T S, Novikova A S, Abramova A M, et al. New-generation low-toxic I-III-VI_2 quantum dots in chemical analysis. J Anal Chem, 2022, 77: 402–409
102 Ding C, Huang Y, Shen Z, et al. Synthesis and bioapplications of Ag_2S quantum dots with near-infrared fluorescence. Adv

Mater, 2021, 33: 2007768
103 Kays J C, Saeboe A M, Toufanian R, et al. Shell-free copper indium sulfide quantum dots induce toxicity in vitro and in vivo. Nano Lett, 2020, 20: 1980–1991
104 Sun B, Najarian A M, Sagar L K, et al. Fast near-infrared photodetection using III-V colloidal quantum dots. Adv Mater, 2022, 34: 2203039
105 Lee K, Park G, Chun B, et al. High-performance InP quantum-dot light-emitting diodes with a NiO_x nanoparticle-embedded hybrid emissive layer. ACS Appl Mater Interfaces, 2025, 17: 1451–1459
106 Lin J, Dai X, Liang X, et al. High-performance quantum-dot light-emitting diodes using NiO_x hole-injection layers with a high and stable work function. Adv Funct Mater, 2020, 30: 1907265
107 Borsoi F, Hendrickx N W, John V, et al. Shared control of a 16 semiconductor quantum dot crossbar array. Nat Nanotechnol, 2024, 19: 21–27
108 Kumar S, Pradhan S. Colloidal quantum dot-based near and shortwave infrared light emitters: recent developments and application prospects. Adv Opt Mater, 2024, 12: 2400993
109 Niu G, Wang L, Gao R, et al. Inorganic halogen ligands in quantum dots: I^-, Br^-, Cl^- and film fabrication through electrophoretic deposition. Phys Chem Chem Phys, 2013, 15: 19595–19600
110 Wang J, Zhang B, Luo J, et al. High performance NIR photodetector with mixed halogen passivation via precursor engineering. Optik, 2022, 266: 169597
111 Lee Y M, Song J H, Jung B K, et al. Cation-exchanged quantum dot-based high-performance near-infrared photodetectors through surface treatment and passivation. Chem Eng J, 2024, 488: 150916
112 Shen W S, Liu Y, Chen X, et al. Metal/organic interface carrier quenching suppression for stable and efficient near-infrared quantum dot light-emitting diodes. Chem Eng J, 2025, 504: 158969
113 Sun Y, Cui G, Guo K, et al. Quantum cascade lasers grown by MOCVD. J Semicond, 2023, 44: 121901
114 Täschler P, Bertrand M, Schneider B, et al. Femtosecond pulses from a mid-infrared quantum cascade laser. Nat Photon, 2021, 15: 919–924
115 Liu S, Wang M, Yu X, et al. Efficient PbSe quantum dot infrared photovoltaic applying MXene modified ZnO electron transport layer. Adv Opt Mater, 2024, 12: 2301252
116 Sergeeva K A, Zhang H, Portniagin A S, et al. The rise of HgTe colloidal quantum dots for infrared optoelectronics. Adv Funct Mater, 2024, 34: 2405307
117 Liu S, Deng C, Wang M, et al. Efficient quantum dot infrared photovoltaic with enhanced charge extraction via applying gradient electron transport layers. Adv Opt Mater, 2024, 12: 2303256